



Classifier-based non-linear projection for adaptive endpointing of continuous speech

Bhiksha Raj^{†§} and Rita Singh[‡]

[†] *Mitsubishi Electric Research Laboratories, Cambridge, MA 02139, U.S.A.,*
[‡] *Carnegie Mellon University, Pittsburgh, PA 15213, U.S.A.*

Abstract

In this paper we present an algorithm for segmenting or locating the endpoints of speech in a continuous signal stream. The proposed algorithm is based on non-linear likelihood-based projections derived from a Bayesian classifier. It utilizes class distributions in a speech/non-speech classifier to project the signal into a 2-dimensional space where, in the ideal case, optimal classification can be performed with a simple linear discriminant. The projection results in the transformation of diffuse, nebulous classes in high-dimensional space into compact clusters in the low-dimensional space that can be easily separated by simple clustering mechanisms. In this space, decision boundaries for optimal classification can be more easily identified using simple clustering criteria. The segmentation algorithm proposed utilizes this property to determine and update optimal classification thresholds continuously for the signal being segmented. The performance of the proposed algorithm has been evaluated on data recorded under extremely diverse environmental noise conditions. The experiments show that the algorithm performs comparably to manual segmentations even under these diverse conditions.

© 2002 Published by Elsevier Science Ltd.

1. Introduction

31 Automatic Speech Recognition (ASR) systems of today have little difficulty in gener-
32 ating good recognition hypotheses for large sections of continuously recorded signals
33 containing speech, when they are recorded in controlled, quiet environments. In such
34 environments silence is easily recognized as such and is clearly distinguishable from
35 speech. However, when the signal is noisy the ASR system is no longer able to clearly
36 discern whether a given segment is speech or noise, and often recognizes spurious words
37 in regions where there is no speech at all. This can be avoided if the beginnings and ends
38 of sections of the signal containing speech are identified prior to recognition and recog-
39 nition is performed only within these boundaries. The process of identification of
40 these boundaries is commonly referred to as endpoint detection or segmentation. While

[§] E-mail: bhiksha@merl.com (B. Raj).

41 there are minor differences in the contexts in which these two terms are used, we will
42 consider them to be synonymous in this paper.

43 Several methods of endpoint detection that have been proposed in the literature. We
44 can roughly categorize them as rule-based methods and classifier-based methods. Rule-
45 based methods use heuristically derived rules relating to some measurable properties of
46 the signal to discriminate between and non-speech. The most commonly used property
47 is the variation in the energy in the signal. Rules based on energy are usually supple-
48 mented by other information such as durations of speech and non-speech events (Lamel
49 *et al.*, 1981), zero crossings (Rabiner and Sambur, 1975), pitch (Hamada *et al.*, 1990),
50 etc. Other notable methods in this category use time-frequency information to locate
51 regions of the signal that can be reliably tagged and then expanded to adjacent regions
52 (Junqua *et al.*, 1994).

53 Classifier-based methods model speech and non-speech events as separate classes
54 and treat the problem of endpoint detection as one of classification. The class distri-
55 butions may be modelled by static distributions such as Gaussian mixtures (e.g. Hain
56 and Woodland, 1998) or by dynamic structures such as hidden Markov models (e.g.
57 Acero *et al.*, 1993). More sophisticated versions use the speech recognizer itself as an
58 endpoint detector. Some endpointing algorithms do not clearly belong to either of the
59 two categories, e.g. those that use only the local variations in the statistical properties of
60 the incoming signal to detect endpoints (Sieglar *et al.*, 1997; Chen and Gopalakrishnan,
61 1998).

62 Rule-based segmentation strategies have two drawbacks. Firstly, the rules are spe-
63 cific to the feature set used for endpoint detection and fresh rules must be generated for
64 every new feature considered. Due to this only a small set of features for which rules are
65 easily derived are used. Secondly, the parameters of the applied rules must be fine tuned
66 to the specific acoustic conditions of the data, and do not easily generalize to other
67 conditions.

68 Classifier-based segmenters, on the other hand, usually consider parametric rep-
69 resentations of the entire spectrum of the signal for endpoint detection. While they
70 typically perform better than rule-based segmenters, they too have some shortcom-
71 ings. They are specific to the kind of recording environments that they have been
72 trained for, e.g. they perform poorly on noisy speech when trained on clean speech,
73 and vice versa. They must therefore be adapted to the current operating conditions.
74 Since the feature representations usually have many dimensions (typically 12–40 di-
75 mensions), adaptation of classifier parameters requires relatively large amounts of
76 data and has not always been observed to result in large improvements in speech/non-
77 speech classification accuracy (Hain and Woodland, 1998). Moreover, when adapta-
78 tion is to be performed, the segmentation process becomes slower and more complex.
79 This can increase the time lag (or *latency*) between the time at which endpoints occur
80 and the time at which they are identified, which might affect runtime implementa-
81 tions. When classes are modelled by dynamical structures such as HMMs, the de-
82 coding strategies used (e.g. Viterbi, 1967) can introduce further latencies. Recognizer-
83 based endpoint detection involves even greater latency since a single pass of recog-
84 nition rarely results in good segmentation and must be refined by additional passes
85 after adapting the acoustic models used by the recognizer. The problems of high
86 dimensionality and higher latency render classifier-based segmentation less effective in
87 many situations. Consequently, classifier-based segmentation strategies are mainly
88 used only in offline (or *batchmode*) segmentation.

89 In this paper we propose a classifier-based method of endpoint detection which is
90 based on non-linear likelihood-based projections derived from a Bayesian classifier. In
91 the proposed method, high-dimensional parametrizations of the signal are projected
92 onto a 2-dimensional space using the class distributions in a speech/non-speech clas-
93 sifier. In this 2-dimensional space the separation between classes is further increased by
94 an averaging operation. Rather than adapting classifier distributions, this algorithm
95 continuously updates the estimate of the optimal classification boundary in this 2-di-
96 mensional space. The performance of the proposed algorithm has been evaluated on the
97 SPINE (SPINE, 2001) evaluation data, which are recorded under extremely diverse
98 environmental noise conditions. The recognition experiments show the method to be
99 highly effective, resulting in minimal loss of recognition accuracy as compared to
100 manually obtained segment boundaries.

101 In the rest of this paper we describe the proposed algorithm and the evaluation
102 experiments in detail. In Section 2 we describe the non-linear projections used by the
103 algorithm. In Section 3 we describe how decision boundaries are obtained for the
104 projected features. In Section 4 we describe two implementations of the segmenter. In
105 Section 5 we describe experimental results and in Section 6 we present our conclusions.

2. Segmentation features

107 In any speech recording, the speech segments differ from non-speech segments in many
108 ways. The energy levels, energy flow patterns, spectral patterns and temporal dynamics
109 of speech are consistently different from those of non-speech. Feature representations
110 used for the purpose of distinguishing speech from non-speech must capture as many of
111 these distinguishing features as possible. For this reason, features used by ASR systems
112 for recognition are particularly suitable. These are typically based on spectral repre-
113 sentations derived from the short-term Fourier transform of the signal and are further
114 augmented by difference features that capture the trends in the basic feature (Rabiner
115 and Juang, 1993). Figure 1 shows scatter plots of the first four dimensions of a typical
116 feature vector used to represent signals in ASR systems. The dark regions in the plots
117 represent non-speech events in the signal, and the light regions represent speech events.
118 In both plots in Figure 1, speech and non-speech are observed to have distinctly dif-
119 ferent distributions.

120 Such feature representations however tend to have relatively high dimensionality.
121 For example, typical cepstral vectors are 13-dimensional which become 26-dimensional
122 when supplemented by difference vectors. When using high-dimensional features for
123 distinguishing speech from non-speech, Bayesian classifiers are usually more effective
124 than rule-based ones. Bayesian classifiers are however fraught with problems. When the
125 test data do not match the training data used to train the classifiers, they perform
126 poorly. To avoid this problem classifier distributions are typically trained using a large
127 variety of data, so that they generalize to a large number of test conditions. However, it
128 is impossible to predict every kind of test condition that may be encountered and
129 mismatches between the test data and the distributions used by the classifier will always
130 occur. To compensate for this, the class distributions must be adapted to the test data.
131 Commonly used adaptation methods are *maximum a posteriori* (MAP) (Duda *et al.*,
132 2000) and Extended MAP (Lasry and Stern, 1984) adaptation, and maximum likeli-
133 hood (ML) adaptation methods such as MLLR (Leggetter and Woodland, 1994). For
134 high-dimensional features both MAP and ML require moderately large amounts of

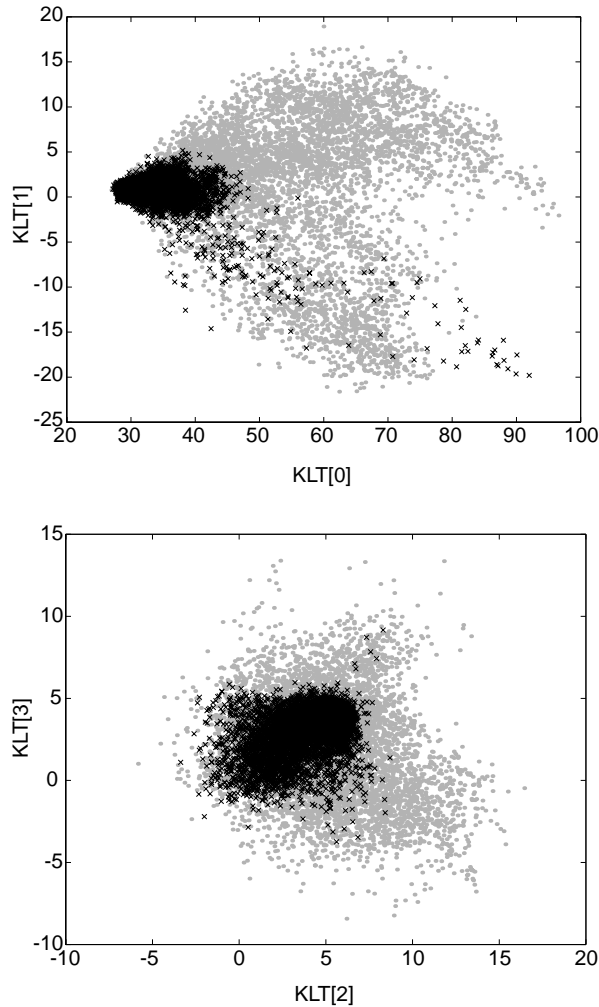


Figure 1. Scatter plot of four components of a typical feature representation of a recorded signal. The feature vectors used in this case were derived by KLT transformation of Mel-frequency log-spectral vectors derived from 25 MS frames of the signal, where adjacent frames overlapped by 15 MS. The left panel shows the scatter of the first two components of the vectors. The right panel shows the scatter of the third and fourth components. In both figures the dark crosses represent vectors from non-speech segments in the signal. The gray points represent vectors from speech segments. The actual scatter of the gray points extends into the black region, but is obscured.

135 data. In most cases, no labelled samples of the test data are available and the adap-
136 tation must therefore be unsupervised. Unsupervised MAP adaptation is generally
137 ineffective (Doh, 2000). Even ML adaptation does not result in large improvements in
138 classification over that given by the original mismatched classifier, for speech/non-
139 speech classification (e.g. Hain and Woodland, 1998). Additionally, for the high-di-
140 mensional features considered, MAP and ML adaptation methods require multiple

141 passes over the data and are computationally expensive. This can be a problem since
142 endpoint detection is usually required to be a low computation task.

143 Many of the problems due to high-dimensional spectral features can be minimized or
144 eliminated by projecting them down to a lower-dimensional space. However, such a
145 projection must retain all classification information from the original space. Linear
146 projections such as the KLT and LDA result in loss of information when the dimen-
147 sionality of the reduced space is too small. We therefore resort to discriminant analysis
148 for a non-linear dimensionality reducing projection that is guaranteed not to result in
149 any loss in classification performance under ideal conditions (Singh and Raj, 2002). In
150 the following subsection we describe this in greater detail.

2.1. Likelihoods as discriminant projections

152 Bayesian classification can be viewed as a combination of a non-linear projection and
153 classification with linear discriminants. When attempting to distinguish between N
154 classes, data vectors are non-linearly projected onto an N -dimensional space, where
155 each dimension is a monotonic function, typically the logarithm, of the probability of
156 the vector (or the probability density value at the vector) for one of the classes. An
157 incoming d -dimensional vector X is thus projected onto an N -dimensional vector Y :

$$\begin{aligned} Y &= [\log(P(X|C_1)) \log(P(X|C_2)) \dots \log(P(X|C_N))] \\ &= [Y_1 Y_2 \dots Y_N], \end{aligned} \quad (1)$$

159 where $\log(P(X|C_i))$ is the log likelihood of the vector X computed using the probability
160 distribution or density of class C_i . This constitutes Y_i , the i th component of Y . Equation
161 (1) defines a *likelihood projection* into a new N -dimensional space of likelihoods. In this
162 space, the optimal classifier between any two classes C_i and C_j is a simple linear dis-
163 criminant of the form

$$Y_i = Y_j + \varepsilon_{i,j}, \quad (2)$$

165 where $\varepsilon_{i,j}$ is an additive constant that is specific to the discriminant for classes C_i and C_j .
166 These linear discriminants define hyperplanes that lie at 45° to the axes representing the two
167 classes. In the N -dimensional space, the decision region for any class C_i is the region
168 bounded by the $N - 1$ hyperplanes

$$Y_i = Y_j + \varepsilon_{i,j}, \quad j = 1, 2, \dots, N, \quad j \neq i. \quad (3)$$

170 The classification error expected from the simple optimal linear discriminants in the like-
171 lihood space is the same as that expected with the more complicated optimal discriminant in
172 the original space (Singh *et al.*, 2001). Thus, when $N < d$, the likelihood projection
173 constitutes a dimensionality reducing projection that accrues no loss whatsoever of
174 information relating to classification.

175 For a two-class classifier, such as a speech/non-speech classifier, the likelihood
176 projection reduces the data to only two dimensions. Figure 2 shows an example of the
177 2-dimensional likelihood projections for the data shown in Figure 1. For a two-class
178 classifier, further dimensionality reduction is possible for no loss of information by
179 projecting the 2-dimensional likelihood space onto the axis defined by

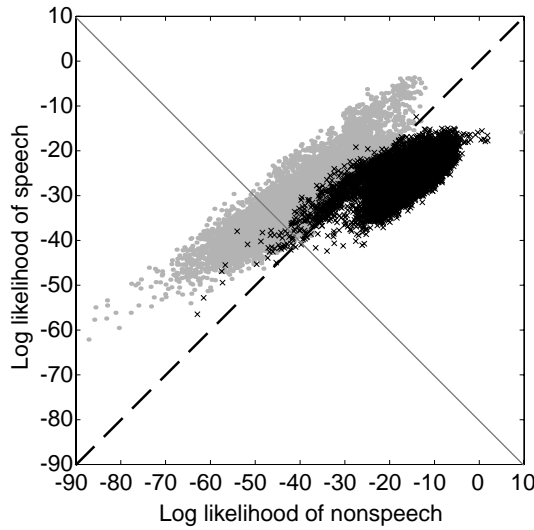


Figure 2. Scatter of the log likelihood of the speech frames computed using the distributions of the non-speech and speech classes. The dotted line shows the optimal linear discriminant between the classes. This discriminant performs exactly as the high-dimensional classifier in the original data space. The solid line shows an axis that is parallel to the one onto which the data are projected to obtain likelihood differences. This is orthogonal to the optimal linear discriminant.

$$Y_1 + Y_2 = 0. \quad (4)$$

181 This axis is orthogonal to the optimal linear discriminant $Y_1 = Y_2 + \varepsilon_{1,2}$. The unit vector \hat{u}
 182 along the axis is $[1/\sqrt{2}, -1/\sqrt{2}]$. The projection Z of any vector $Y = [Y_1, Y_2]$, derived
 183 from a high-dimensional vector X , onto this axis can be computed as $\sqrt{2}Y \cdot \hat{u}$, which is
 184 given by

$$Z = Y_1 - Y_2 = \log(P(X|C_1)) - \log(P(X|C_2)). \quad (5)$$

186 The multiplicative factor of $\sqrt{2}$ has been introduced in the projection for simplification and
 187 does not affect classification as it merely results in a scaling of the projected features. Figure
 188 3 shows the histograms of such a 1-dimensional projection of the speech and non-speech
 189 vectors in the signal used in Figure 1. Figure 4 shows the combined histogram of the speech
 190 and non-speech data. From these figures we observe that both the speech and non-speech
 191 data have distinctive, largely connected distributions. Further the combined histogram shows
 192 a clear inflexion point between the two, the position of which actually defines the optimal
 193 classification threshold between speech and non-speech.

194 The optimal linear discriminant in the 2-dimensional likelihood projection space is
 195 guaranteed to perform as well as the optimal classifier in the original multidimensional
 196 space only if the likelihoods of the classes are computed using the *true* distribution (or
 197 density) of the two classes. When the distributions used for the projection are not the
 198 true distributions, the classification performance of the optimal linear discriminant on
 199 the projected data is nevertheless no worse than the classification performance obtainable
 200 using *these* distributions in the original high-dimensional space (Singh *et al.*,

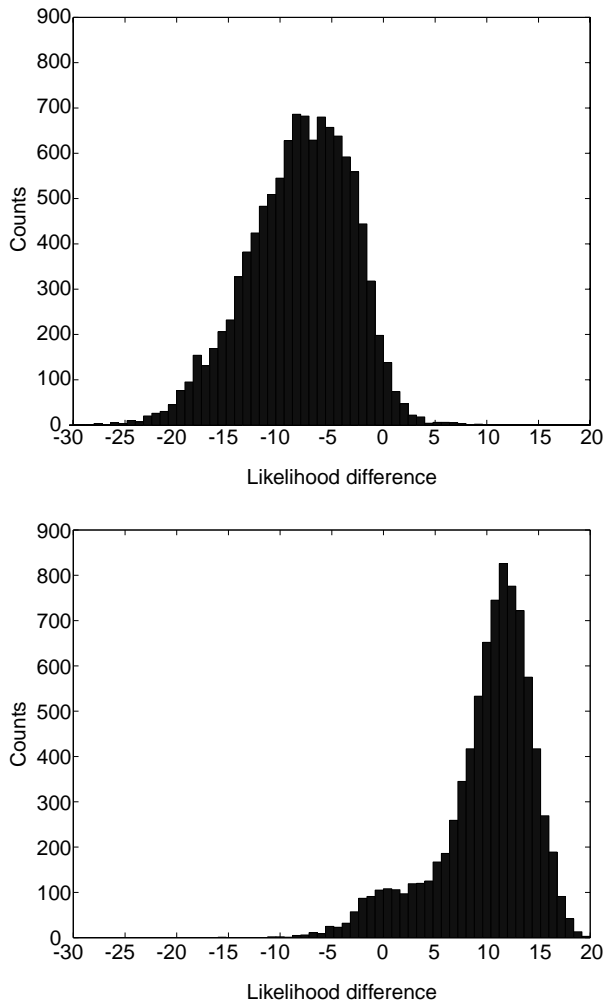


Figure 3. The left panel shows the histogram of the likelihood-difference values of frames of speech. The right panel shows a similar histogram for frames of non-speech signals. The data used for both plots have been sampled from the SPINE1 training corpus.

201 2001). However, the optimal linear discriminant for the test data may not be easily
202 determinable. Figure 5a illustrates this problem. through an example where the dis-
203 tributions of the likelihood-difference features for speech and non-speech overlap to
204 such a degree that the likelihood-difference histogram exhibits only one clear mode. The
205 threshold value corresponding to the optimal linear discriminant cannot therefore be
206 determined from this distribution. Clearly, the classes need to be separated further in
207 order to improve our chances of locating the optimal decision boundary between them.
208 In the following subsection we describe how the separation between the classes in the
209 space of likelihood differences can be increased by an averaging operation.

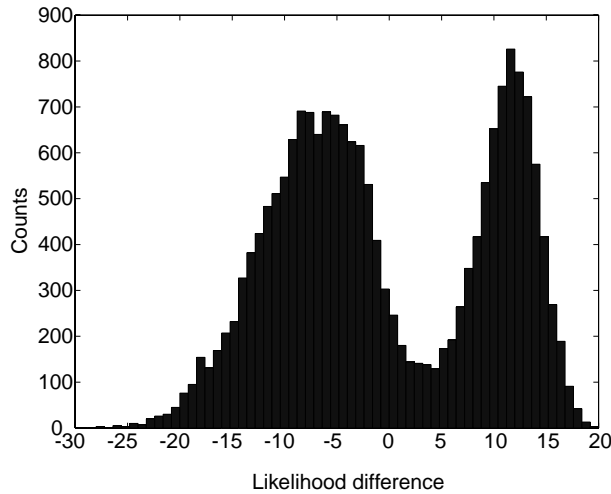


Figure 4. The histogram of likelihood differences for the combined speech and non-speech data used in Figure 3.

2.2. The effect of averaging on the separation between classes

211 Let us begin by defining a measure of the separation between two classes. Given two
 212 classes C_1 and C_2 of a scalar random variable Z , whose means are given by μ_1 and μ_2
 213 and variances by V_1 and V_2 , respectively. We can define a function $F(C_1, C_2)$ as

$$F(C_1, C_2) = \frac{(\mu_1 - \mu_2)^2}{c_1 V_1 + c_2 V_2}, \quad (6)$$

215 where c_1 and c_2 are the fraction of data points in classes C_1 and C_2 , respectively. This ratio is
 216 analogous to the criterion, sometimes called the *Fischer ratio* or the *F-ratio*, used by the
 217 Fischer linear discriminant (Duda *et al.*, 2000) to quantify the separation between two
 218 classes. We will therefore also refer to the quantity in Equation (6) as the *F-ratio* in the
 219 rest of this paper. The difference between the Fischer ratio and Equation (6) is that
 220 Equation (6) is stated in terms of variances and fractions of data, rather than scatters.
 221 Like the Fischer ratio, the *F-ratio* in Equation (6) is a good measure of the separation
 222 between classes – the larger the ratio the greater the separation, and vice versa.

223 Consider a new random variable \bar{Z} that has been derived from Z by replacing every
 224 sample of Z by the weighted average of K samples of Z , all of which are taken from a
 225 single class, either C_1 or C_2 . The new random variable is given by

$$\bar{Z} = \sum_{i=1}^K w_i Z_i, \quad (7)$$

227 where Z_i is the i th sample of Z used to obtain \bar{Z} , $0 \leq w_i \leq 1$, and the weights w_i sum to 1.
 228 Since all the samples of Z that were used to construct any sample of \bar{Z} come from the
 229 same class, that sample of \bar{Z} is associated with that class. Thus all samples of \bar{Z} cor-
 230 respond to either C_1 or C_2 . The mean of the samples of \bar{Z} that correspond to class C_1 is
 231 now given by

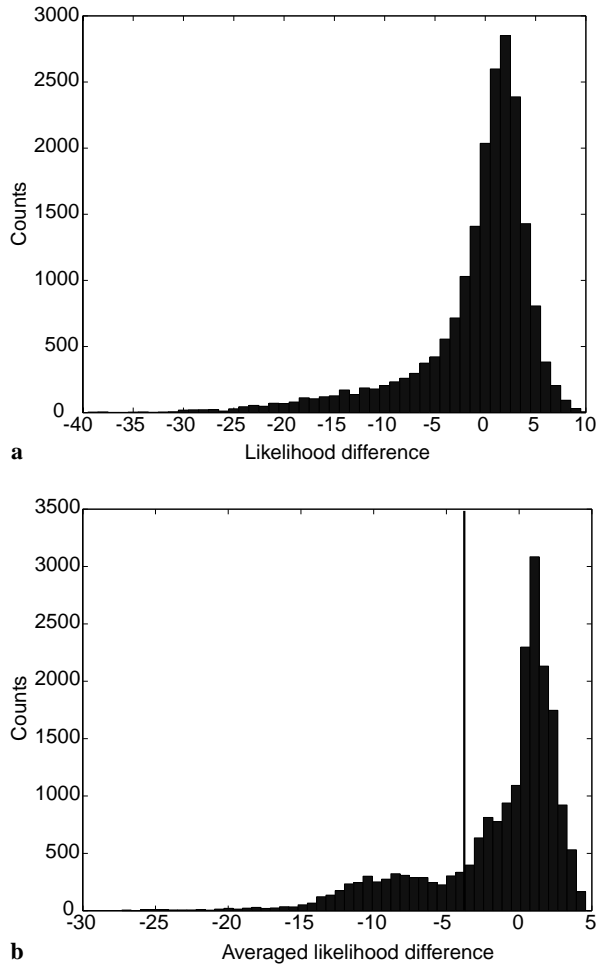


Figure 5. (a) A histogram of likelihood differences for a signal where the speech mode and non-speech mode overlap so the extent that the overall histogram has only one mode. (b) The histogram of the averaged likelihood differences for the data from (a). The speech and non-speech modes are now clearly visible. The vertical line shows the empirically determined optimal classification boundary between the two classes. The optimal threshold is very close to the inflexion point.

$$\bar{\mu}_1 = E(\bar{Z}|C_1) = \sum_{i=1}^K w_i E(Z|C_1) = \mu_1. \quad (8)$$

233 The mean of class C_2 is similarly obtained as $\bar{\mu}_2 = \mu_2$. The variance of the samples of \bar{Z}
 234 belonging to class C_1 is given by

$$\begin{aligned} \bar{V}_1 &= E\left(\left(\sum_{i=1}^K w_i Z_i - \mu_1\right)^2\right) = E\left(\left(\sum_{i=1}^K w_i (Z_i - \mu_1)\right)^2\right) \\ &= \sum_{i=1}^K \sum_{j=1}^K w_i w_j E((Z_i - \mu_1)(Z_j - \mu_1)) \\ &= V_1 \sum_{i=1}^K \sum_{j=1}^K w_i w_j r_{ij} = \beta V_1, \end{aligned} \quad (9)$$

10

B. Raj and R. Singh

236 where r_{ij} is the relative covariance between Z_i and Z_j and β represents the summation term.
237 It is easy to show from basic arithmetic principles that, since the weights sum to 1,

$$\sum_{i=1}^K \sum_{j=1}^K w_i w_j = \left(\sum_{j=1}^K w_j \right)^2 = 1. \quad (10)$$

239 Since $0 \leq w_j \leq 1$ and $|r_{ij}| \leq 1$, it follows that

$$\sum_{i=1}^K \sum_{j=1}^K w_i w_j r_{ij} \leq 1. \quad (11)$$

241 From Equations (9) and (11) it is clear that

$$\bar{V}_1 \leq V_1. \quad (12)$$

243 Thus, the variance of class C_1 for \bar{Z} is no greater than that for Z . Similarly, $\bar{V}_2 \leq V_2$. Hence,

$$c_1 \bar{V}_1 + c_2 \bar{V}_2 = \beta(c_1 V_1 + c_2 V_2), \quad (13)$$

245 where $\beta \leq 1$. The F -ratio of the classes for the new random variable \bar{Z} is given by

$$\bar{F}(C_1, C_2) = \frac{(\bar{\mu}_1 - \bar{\mu}_2)^2}{c_1 \bar{V}_1 + c_2 \bar{V}_2} = \frac{(\mu_1 - \mu_2)^2}{\beta(c_1 V_1 + c_2 V_2)} = \frac{F(C_1, C_2)}{\beta}. \quad (14)$$

247 If we can ensure that β is less than 1, then the F -ratio of the averaged random variable \bar{Z} is
248 greater than that of the original random variable Z . It is clear from Equation (11) that β
249 is less than 1 if even one of the various r_{ij} values is less than 1.

250 This fact can be used to improve the separation between speech and non-speech
251 classes in the likelihood space by representing each frame by the weighted average of
252 the likelihood-difference values of a small window of frames around that frame, rather
253 than by the likelihood difference itself. Since the relative covariances between all the
254 frames within the window are not all 1, the β value for the new averaged likelihood-
255 difference feature is also less than 1. If the likelihood-difference value of the i th frame is
256 represented as L_i , the averaged value is given by

$$\bar{L}_i = \sum_{j=-K_1}^{K_2} w_j L_{i+j}. \quad (15)$$

258 Figure 5b shows the histogram of the averaged likelihood-difference features for the data in
259 Figure 5a. We observe that the speech and non-speech are indeed more separable in Figure
260 5b than in Figure 5a. In fact, the averaging operation improves the separability between the
261 classes even when applied to the 2-dimensional likelihood space. Figure 6 shows the scatter
262 of the averaged likelihoods for the data used in Figure 2. Comparison of the two figures
263 shows that the averaging has indeed improved the separation between classes greatly even in
264 the 2-dimensional space.

265 One of the criteria for averaging to improve the F -ratio is that *all* the samples within
266 the window that produces the averaged feature must belong to the same class. For a

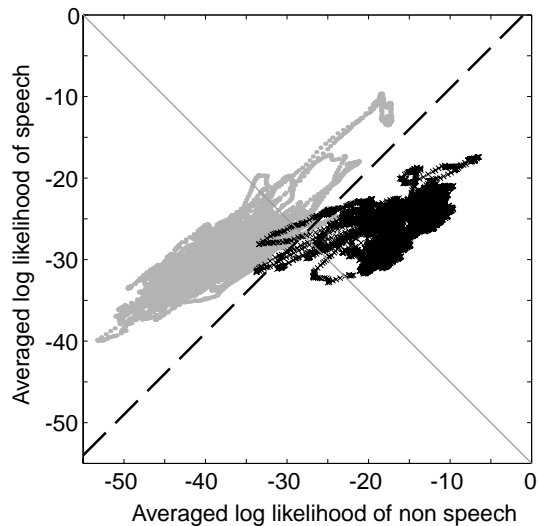


Figure 6. The scatter of averaged likelihoods for the data from Figure 2. The dotted line shows the best linear discriminant with slope 1 between the two classes. The classification error obtained with this discriminant is 1.3%. The optimal classification error for the original (unaveraged) data was 7.4%. Better linear discriminants are possible if the slope is allowed to vary from 1. For the data in this figure, the optimal linear discriminant of any slope, which has not been shown here, has a slope of 0.83 and results in an error rate of only 0.9%.

267 continuous signal there is no way of ensuring that any window contains only the same
268 class of signal. However in any recording, speech and non-speech frames do not occur
269 randomly. Rather they occur in contiguous blocks. As a result, except for the tran-
270 sition points between speech and non-speech, which are relatively infrequent in com-
271 parison to the actual number of speech and non-speech frames, most windows of the
272 signal contain largely one kind of signal, provided they are sufficiently short. Thus, the
273 averaging operation results in an increase in the separation between speech and non-
274 speech classes in most signals. For example, the averaged likelihoods computed for the
275 histogram in Figure 5b were, in fact, computed on the continuous signal without seg-
276 regating speech and non-speech segments. We observe that the averaging results in an
277 increased separation between speech and non-speech classes even in this case. Note that
278 an averaging operation would not achieve any increase in the separation between
279 classes if speech and non-speech frames were randomly interspersed in the incoming
280 signal.

281 In this paper we therefore use the averaged likelihood-difference features to represent
282 frames of the signal to be segmented. In the following sections we address the problem
283 of determining which frames represent speech, based on these 1-dimensional features.

3. Threshold identification for endpoint detection

285 The histograms of averaged likelihood-difference values typically exhibit two distinct
286 modes, with an inflexion point between the two. One of the modes represents the
287 distribution of speech, and the other the distribution of non-speech. An example in

288 shown in Figure 5b. The location of the inflexion point between the two modes ap-
 289 proximately represents the optimal decision threshold where the two distributions
 290 crossover. This, however, is not easy to locate, since the histogram is, in general, not
 291 smooth, and has many minor peaks and valleys as can be seen in Figure 5b. For this
 292 reason, the problem of finding the inflexion point is not merely one of finding the
 293 minimum. In the following subsections we propose two methods of identifying the
 294 location of inflexion points in the histograms: Gaussian mixture fitting and polynomial
 295 fitting.

296 We note here that bimodal distributions are also exhibited by the energy of the
 297 speech frames. This has previously been exploited for endpoint detection and noise
 298 estimation. For example, Hirsch (1993) and Compernelle (1989), base the estimate of
 299 SNR and the presence of the speech signal based on the relative distance between the
 300 two modes. Several researchers (e.g. Cohen, 1989) have used the distance between the
 301 modes in the histogram of frame energies to estimate SNR. While these approaches
 302 look similar to the one suggested in this paper, the similarity between the two is only
 303 very superficial.

3.1. Gaussian mixture fitting

305 In Gaussian mixture fitting we model the distribution of the smoothed likelihood dif-
 306 ference features of the signal as a mixture of two Gaussians, one of which is expected to
 307 capture the speech mode, and the other the non-speech mode. The mixture weights,
 308 means, and variances of the two Gaussians, represented as c_1, μ_1, V_1 and c_2, μ_2, V_2 , are
 309 computed using the expectation maximization (EM) algorithm (Dempster *et al.*, 1977).
 310 The decision threshold is estimated as the point at which the two Gaussians crossover.
 311 This point is obtained as the solution to the equation

$$\frac{c_1}{\sqrt{2\pi V_1}} \exp\left(\frac{-(x - \mu_1)^2}{2V_1}\right) = \frac{c_2}{\sqrt{2\pi V_2}} \exp\left(\frac{-(x - \mu_2)^2}{2V_2}\right). \quad (16)$$

313 By taking logarithms on both sides, this reduces to the quadratic equation

$$\frac{(x - \mu_1)^2}{2V_1} - \log(c_1) + 0.5 \log(V_1) = \frac{(x - \mu_2)^2}{2V_2} - \log(c_2) + 0.5 \log(V_2) \quad (17)$$

315 only one of whose two solutions lies between μ_1 and μ_2 . This is the estimated decision
 316 threshold.

317 The dotted contours in Figure 7 show the Gaussian mixture fit to the histogram in
 318 Figure 5b. The thin dotted contours show the individual Gaussians in the fit. The
 319 crossover point, marked by the rightmost dotted vertical line, is the estimate of the
 320 optimum decision threshold. We observe that the value of the estimated threshold is
 321 greater than the true optimum decision threshold, which would result in many more
 322 non-speech frames being tagged as speech frames as compared to the optimum decision
 323 threshold. This happens when the speech and non-speech modes are well separated. On
 324 the other hand, Gaussian mixture fitting is very effective in locating the optimum de-
 325 cision threshold in cases where the inflexion point in the histogram does not represent a
 326 local minimum. Figure 8 shows such an example.

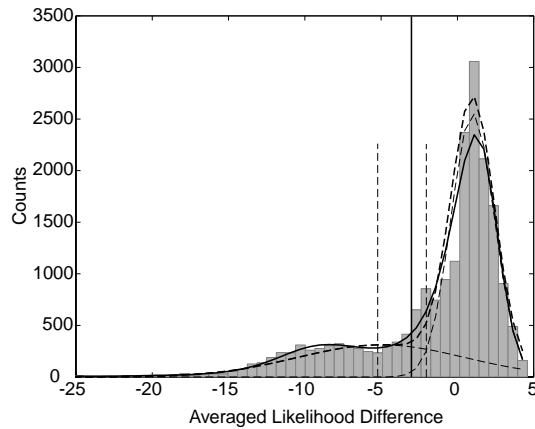


Figure 7. This figure shows the Gaussian and polynomial fits to the histogram in Figure 5b. The thin dotted lines show the individual Gaussians in the Gaussian fit. The thicker dotted line shows the overall Gaussian fit. The solid line shows the polynomial fit to the histogram. The long vertical line shows the empirically determined optimal classification threshold. The shorter vertical dotted lines show the classification thresholds given by the polynomial and Gaussian fits.

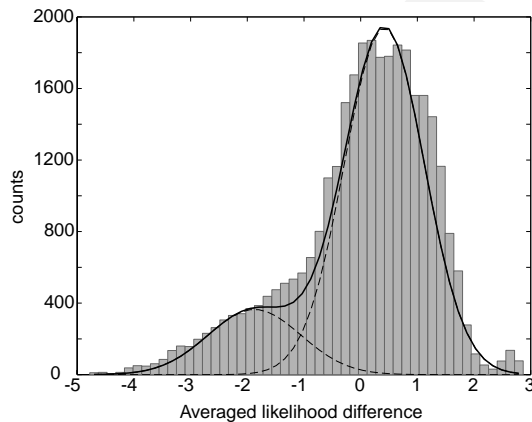


Figure 8. The histogram of the averaged likelihood differences for a signal where the speech and non-speech modes are so close that there is no local minimum between the two. Nevertheless a Gaussian fit to the distribution is successful at locating the classification threshold between the two. The two dotted curves show the two Gaussians in the fit. The solid line shows the overall Gaussian fit. The crossover point between the two Gaussians is the determined decision threshold.

3.2. Polynomial fitting

328 In polynomial fitting we obtain a smoothed estimate of the contour of the histogram
 329 using a polynomial. Due to inherent irregularities, direct modelling of the histogram
 330 contour as a polynomial frequently fails to capture the true underlying points of the
 331 histogram effectively. We therefore fit a polynomial to the *logarithm* of the histogram,
 332 with all bins incremented by 1 prior to the logarithm.

333 Let h_i be the value of the i th bin in the histogram. We estimate the coefficients of the
334 polynomial

$$H(i) = a_K i^K + a_{K-1} i^{K-1} + \dots + a_1 i + a_0, \quad (18)$$

336 where K is the polynomial order and a_K, a_{K-1}, \dots, a_0 are the coefficients that minimize
337 the error

$$E = \sum_i (H(i) - \log(h_i + 1))^2. \quad (19)$$

339 Optimizing E for the a_j values results in a set of linear equations that can be easily
340 solved. The smoothed fit to the histogram can now be obtained from $H(i)$ by reversing
341 the log and addition by 1 operations as

$$\tilde{H}(i) = \exp(H(i)) - 1 = \exp(a_K i^K + a_{K-1} i^{K-1} + \dots + a_1 i + a_0) - 1. \quad (20)$$

343 The thick contour in Figure 7 is the smoothed contour of the histogram obtained using
344 a sixth-order polynomial fit. We see that the polynomial fit models the contours of the
345 histogram very well. Identifying the inflexion point is now merely a question of locating
346 the minimum value of this contour. Note that the exponentiation in Equation (20) is
347 not necessary for locating the inflexion point, which can be located on $H(i)$ itself. Since
348 the polynomial is defined on the indices of the histogram bins, rather than on the
349 centres of the bins, the inflexion point gives us the index of the histogram bin within
350 which the inflexion point lies. The centre of this bin gives us the optimum decision
351 threshold. In histograms where the inflexion point does not represent a local minimum,
352 other simple criteria such as higher order derivatives must be used.

4. Implementation of the segmenter

354 In this section we describe two implementations of the segmenter: batchmode and run-
355 time. In the former, endpointing is done on pre-recorded signals and real-time con-
356 straints do not apply. In the latter, the endpointer must identify beginnings and ends of
357 speech segments with minimal delay in identification, and therefore must have minimal
358 dependence on future samples of the signal.

359 In both implementations, using a suitable initial feature representation, likelihood
360 difference features are first derived for each frame of the signal. From these, averaged
361 likelihood-difference features are computed using Equation (15). The averaging window
362 can be either symmetric (i.e. $K_1 = K_2$ in Equation (15)) or asymmetric ($K_1 \neq K_2$), de-
363 pending on the implementation. The window length ($K_1 + K_2 + 1$) is typically 40–50
364 frames. Its shape can differ, but we have found rectangular or Banning windows to be
365 particularly effective. Rectangular windows have been observed to be more effective
366 when inter-speech silences are long, whereas the Hanning window is more effective
367 when shorter gaps are expected. The resulting sequence of averaged likelihood differ-
368 ences is used for endpoint detection.

369 Each frame is now classified as speech or non-speech by comparing its averaged
370 likelihood-difference against a threshold that is specific to the frame. The threshold for
371 any frame is obtained from a histogram computed over a segment of the signal span-
372 ning several 1000 frames that includes that frame. The exact placement of this segment

373 is dependent on the type of implementation. Once all frames are tagged as speech or
374 non-speech, contiguous segments of speech that lie within a small number of frames of
375 each other are merged. Speech segments that are shorter than 10 MS are discarded.
376 Finally, all speech segments are padded at the beginning and the end by about half the
377 size of the averaging window.

4.1. Batchmode implementation

379 In batchmode implementation the entire signal is available for processing. Data from
380 both, the past and the future of any segment of the signal can be used when classifying
381 that segment. In this case the main goal is to extract entire utterances of speech from the
382 continuous signal. Here the window used to obtain the averaged likelihood difference is
383 a symmetric rectangular window, about 50 frames wide. The histogram used to com-
384 pute the threshold for any frame is derived from a segment of signal *centered* around
385 that frame. The length of this segment is about 50 s when the background noise con-
386 ditions are expected to be reasonably stationary, and shorter otherwise. We have found
387 segment lengths shorter than 30 s to be inadequate. Merging of adjacent segments and
388 padding of speech segments on either side is performed after the classification as a post-
389 processing step.

4.2. Runtime implementation

391 Runtime implementation is aimed at applications that require an endpoint detector for
392 continuous listening. In such situations one cannot afford delays of more than a frac-
393 tion of a second before determining whether the incoming signal is within a speech
394 segment or not. The various parameters of the segmenter must be suitably adapted to
395 the situation. For runtime implementation the averaging window is asymmetric, but
396 remains 40–50 frames wide. The weighting function is also asymmetric. An example of
397 a function that we have found to be effective is one constructed using two unequal
398 Hanning windows. The lead portion of the window, that covers frames to the future of
399 the current frame, is half of an 8 frame wide Hanning window and covers four frames.
400 The lag portion of the window, that applies to frames from the past, is the initial half of
401 a 70–90 frame wide Hanning window, and covers between 35 and 45 frames. We note
402 here that any similar skewed window may be applied.

403 The histogram used for determining decision thresholds for any frame is computed
404 from the 30 to 50 s long segment of the signal immediately prior to, and including, the
405 current frame. When the first frame that is classified as speech is located, the beginning
406 of a speech segment is marked as having begun half a (averaging) window size number
407 of frames prior to it. The end of a speech segment is marked at the halfway point of the
408 first window size length sequence of non-speech frames following a speech frame.

5. Experimental results

410 In this section we describe a set of experiments which we conducted to test the end-
411 pointing/segmentation strategy proposed in this paper. Both batchmode and runtime-
412 type implementations were evaluated using the CMU SPHINX speech recognition
413 system. We first describe the databases that we chose to use for our experimentation.
414 We then describe the features computed and other implementation details that were

415 specific to the experiments. Finally, we present the experimental results and our con-
416 clusions.

5.1. Databases used

418 The databases chosen for experiments were the “Speech in noisy environments” SPINE1
419 and SPINE2 databases provided by LDC (Linguistic Data Consortium, 2001). These data-
420 bases were used by the Naval Research Labs in the years 2000 and 2001 as training, de-
421 velopment and test data for the first and second SPINE evaluations (SPINE, 2001). The
422 databases contain speech recorded over a variety of moderate to severe environmental noise
423 conditions of the type encountered in real military environments, such as tanks, helicopters,
424 aircraft carriers, military vehicles, airplanes, etc. The speaking styles are also characteristic
425 of those of military personnel communicating in highly unpredictable and reaction-pro-
426 voking situations involving tracking and sighting of targets, ambush and evasion. The
427 speech forms are highly spontaneous, with laughter, shouting, screaming, etc. Additionally,
428 in SPINE1 data, several recordings have multiple energy levels introduced due to a com-
429 bination of continuous recording and push-button activation of the communication channel.
430 When the channel is not open the recording equipment records only equipment noise. When
431 the button is pushed to open the communication channel, channel and background noises,
432 sometimes at high ambient levels, begin to get recorded. Multiple utterances with inter-
433 utterance silences can be recorded within one push-button episode. Energy based segmen-
434 tation is especially difficult in such cases since the energy level trajectory at the sudden
435 onset of the second level of background noise mimics the trajectories expected when speech
436 sets in (Singh *et al.*, 2001).

437 The SPINE2 database is in general noisier than the SPINE1 database. The lower
438 panel in Figure 9 shows a typical noisy utterance from the SPINE2 evaluation database.
439 The estimated SNR of this signal is approximately 0dB. The SNR is low enough to
440 obscure some of the episodes of speech completely. All SPINE1 recordings are 16 KHz
441 sampled wideband speech. The SPINE2 database has two components: 16 KHz wide-
442 band speech and coded speech that has been obtained by low pass filtering the signals
443 from the first component to telephone bandwidth and passing them through one of
444 several codecs. Specifically, the MELP, CELP, CVSD and LPC codecs (DDVPC, 2001)
445 have been used in the evaluation data. The codecs introduce high levels of distortion
446 that degrade the signal, making it more difficult both to locate the endpoints of the data
447 and to recognize it. The endpointing algorithm presented in this paper was evaluated
448 against both the wideband and the coded narrowband components of the SPINE2
449 evaluation data.

5.2. Feature representation and implementation details

451 All signals were windowed into 25 MS frames, where adjacent frames overlapped by
452 15 MS. For wideband data a bank of 40 Mel filters covering the frequency range 130–
453 6800 Hz was used to derive a 40-dimensional log-spectral vector for each frame. For
454 coded speech a bank of 32 Mel filters covering the range 200–3400 Hz was used to derive
455 32-dimensional log-spectral vectors. The Mel-frequency log spectral vectors were then
456 projected down to a 13-dimensional feature vector using the Karhunen Loeve Trans-
457 form (KLT). The eigenvectors for the KLT were computed from the log-spectral vec-
458 tors of clean (office and quiet environment) components of the SPINE2 training corpus.

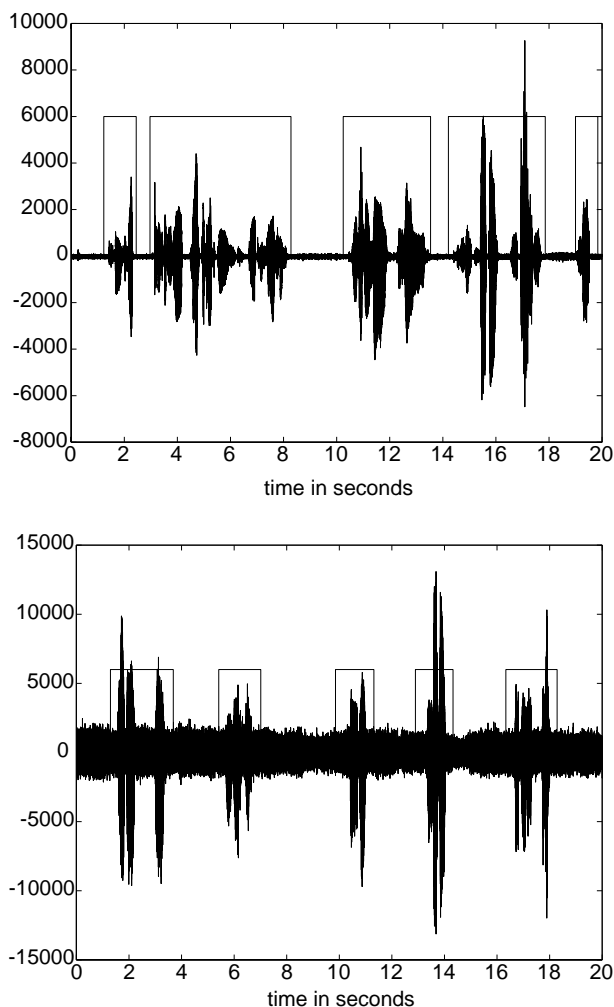


Figure 9. Two examples of segmentations computed by the proposed segmenter. The upper panel shows a relatively clean signal with a global SNR of 20 dB, recorded in an office environment. The lower panel shows a segment of signal with a global SNR of about 0 dB. This signal was recorded in the presence of background operating noise from a Bradley military vehicle.

459 For the coded data they were computed from low-pass filtered and down-sampled
460 versions of the same dataset (uncoded speech). The 13-dimensional KLT-based feature
461 vector for every frame was augmented by a difference feature vector computed as the
462 difference between the feature vectors of the subsequent and previous frames. The final
463 feature vector for any frame thus had 26 components.

464 The 26-dimensional features were then projected down to a 2-dimensional likelihood
465 space using distributions of speech and non-speech estimated from the training corpus.
466 For all experiments with wide-band data, the non-speech distribution used for the
467 likelihood-based projection was trained on several different noise types from the
468 SPINE2 training data. The speech distribution was trained with speech segments from

469 clean (office environments) recordings in the SPINE2 training data. It was empirically
470 observed that training the speech distributions on purely speech data (i.e. without
471 within-utterance silences) resulted in the best segmentation performance. The speech
472 used to train the speech distributions was therefore selected by force-aligning the
473 training data to their transcripts using a recognizer and excising all identified within-
474 utterance silences. For experiments with coded data, separate distributions were trained
475 for each type of codec. For each codec the speech and non-speech distributions were
476 trained with clean speech and noise segments from the SPINE2 training corpus that had
477 been coded using the same codec. All distributions were modelled as mixtures of 32
478 Gaussians, the parameters of which were computed using the EM algorithm. Mixtures
479 of 32 Gaussians were found to be optimal for the task.

480 Likelihood-difference features were then computed by subtracting the likelihood of
481 non-speech from that of speech and windowing and averaging them using Equation
482 (15) to result in the final averaged likelihood difference feature. For experiments with
483 the batchmode implementation, a symmetric rectangular window 50 frames wide was
484 used for this purpose. For the runtime implementation the asymmetric window describe
485 in Subsection 4.2 was used.

486 The classification threshold for any frame was estimated from histograms that were
487 computed from 60 s segments of speech centered at that frame, in the batchmode im-
488 plementation. For frames near the beginning or end of any recording, the first 60 or the
489 last 60 s of the recording were used. For the runtime implementation of the segmenter,
490 the classification threshold for any frame was found using a histogram computed from
491 the 50 s of speech immediately preceding and including the current frame. For frames
492 within 50 s of the beginning of any recording all frames from the beginning until the
493 current frame were used to compute the histogram. For the first 15 s of any recording
494 there were insufficient frames to compute proper histograms, and therefore a default
495 threshold of 0 was used. Figure 9 shows two examples of segmentations obtained using
496 the batchmode segmenters for wideband speech. The segmenter is observed to have
497 accurately captured speech segments in both the noisy and clean signals.

5.3. Results

499 Table I shows the accuracy with which frames have been identified as speech or non-
500 speech for both, the wideband speech and the coded speech. These accuracies have been
501 measured on a per-frame basis. The reference tags in this case were obtained from the

TABLE I. Classification accuracy of speech and non-speech frames using averaged likelihood difference features and Gaussian-fit based classification threshold estimates

Data type	Segmentation type	Classification accuracy for speech (%)	Classification accuracy for non-speech (%)
Wideband	Batchmode	91.6	90.4
Wideband	Runtime	92.1	86.7
Coded	Batchmode	92.7	82.0

Only raw classification accuracy is reported, and the effect of merging of close segments or deletion of short segments has not been taken into account.

502 manual endpoints, and all frames within an utterance of speech were tagged as speech.
503 Thus, any within-utterance silence frame, even when correctly identified by the classifier
504 as silence, is counted as an error. The accuracies reported in Table I are therefore lower
505 than the true accuracies. Classification accuracy is seen to be better for batchmode
506 implementation than for runtime implementation, and better for wideband speech than
507 coded speech. The classification accuracy of speech is generally higher than that of non-
508 speech. Many of the classification errors do not result in segmentation errors since they
509 are either misclassifications of isolated or short segments of speech frames within ut-
510 terances, which get retagged as speech when segments are merged, or similar segments
511 of silence which, although tagged as speech by the classifier, get discarded due to the
512 short duration of the segments. On the whole, frame-level classification accuracy is not
513 fully indicative of the recognition accuracy to be obtained with the segmenter.

514 The performance of the endpointing algorithm is better measured in terms of the
515 recognition accuracy obtained using its output. Recognition performance is dependent
516 on obtaining complete speech segments, rather than accurate frame-level classification.
517 Table II shows recognition error rates obtained using the various modes of the seg-
518 menter on the SPINE1 data. Tables III and IV show similar results for the SPINE2
519 data. The first row in all tables shows the recognition performance obtained with
520 manually marked endpoints. For the wideband speech, the performances obtained with
521 an energy-based segmenter and a simple classifier-based segmenter are also shown. The
522 energy-based segmenter was based on the algorithm described by Lamel *et al.* (Lamel *et*
523 *al.*, 1981). The classifier-based segmentation was performed by classifying signal frames
524 directly using the distributions used for the projection and *a posteriori* probabilities for
525 the probabilities that were estimated on a set of held out data. Segments were merged
526 using the same criteria that were used by the proposed likelihood-projection based
527 segmenter.

528 The column labelled “Mode” in the tables refers to the specific implementation of the
529 segmenter (either batchmode or runtime). The “Threshold” column refers to the method of
530 identifying classification thresholds. Segmentation errors introduce two types of recognition
531 errors. The first, called *gap insertions*, are spurious words hypothesized by the recognizer
532 in non-speech regions, which have been wrongly tagged as speech by the segmenter. The
533 second are errors that occur due to deletions of speech by the segmenter. The final
534 column in Tables II–IV show gap insertions. Not surprisingly, there are no gap in-
535 sertions when endpoints are manually tagged. Differences between the error rates with
536 manual and automatic endpointing, which are not accounted for by gap insertions, are
537 largely due to deletions by the segmenter. In all test sets, the proposed endpointing

TABLE II. Recognition accuracy obtained on wideband SPINE1 evaluation data that have been segmented using several different methods

Segmenter	Mode	Threshold	Error rate (%)	Gap insertions (%)
Manual endpoints			27.9	0
Proposed algorithm	Batchmode	Gaussian	29.2	0.6
		Polynomial	29.5	0.9
	Runtime		30.0	1.3
Energy-based			35.7	7.2
Classifier-based			37.1	9.1

Gap insertions reflect errors introduced due to spurious non-speech segments that have been identified as speech and recognized.

TABLE III. Recognition accuracy obtained on wideband SPINE2 evaluation data that have been segmented using several different methods

Segmenter	Mode	Threshold	Error rate (%)	Gap insertions (%)
Manual endpoints			47.4	0
Proposed algorithm	Batchmode	Gaussian	48.4	0.7
		Polynomial	48.0	0.7
	Runtime		49.0	0.8
Energy-based			55.7	8.1
Classifier-based			57.9	10.5

Gap insertions reflect errors introduced due to spurious non-speech segments that have been identified as speech and recognized.

TABLE IV. Recognition accuracy obtained on coded SPINE2 evaluation data

Segmenter	Mode	Threshold	Error rate (%)	Gap insertions (%)
Manual endpoints			55.7	0
Proposed algorithm	Batchmode	Polynomial	57.9	1.9

Gap insertions reflect errors introduced due to spurious non-speech segments that have been identified as speech and recognized.

538 algorithm is observed to outperform both energy-based endpointing and classifier-
539 based endpointing by a large margin. Even on coded speech, the performance of the
540 endpointer is very close to that obtained with manually-tagged endpoints, although the
541 overall recognition accuracy is rather worse than that of wideband speech.

542 From Tables II and III we observe that while polynomial-based threshold detection
543 performs better on the SPINE2 set, Gaussian-based threshold detection is superior for
544 the SPINE1 set. The reason for this is that the SPINE1 data were less matched to the
545 distributions used for the likelihood projection (which were trained with SPINE2 data)
546 and so the distribution of averaged likelihood-differences frequently did not exhibit
547 clear local minima at the points of inflexion (e.g. Figure 8). Here, as expected, the
548 Gaussian based threshold detection mechanism was better able to locate thresholds.
549 For the SPINE2 data, histograms typically showed clear local minima between modes.
550 Here, (e.g. Figure 7) Gaussian-based threshold detection tended to overestimate the
551 threshold value (thereby classifying more non-speech frames as speech) and the poly-
552 nomial based method performed better. Gap insertions remained few in all cases. We
553 note that the gap insertion percentage is sometimes larger than the difference between
554 the performances obtained with automatic and manual endpoints. This is because the
555 automatically obtained endpoints sometimes resulted in slightly fewer recognition er-
556 rors in true speech segments than the manually determined endpoints. This is an artifact
557 of the manner in which recognition is performed in the SPHINX, which expects a short
558 amount of silence at beginnings and ends of utterances.

559 In Tables II and III, the runtime segmenter is observed to be slightly worse than the
560 batchmode segmenter in all cases. However, the degradation from batchmode to run-
561 time segmentation is not large. During our experiments we also observed that the
562 segmenter performed better under conditions of mismatch between projecting distri-
563 butions and the data when speech distributions were computed using clean speech,
564 rather than an assortment of noisy speech. Finally, as measured in our experiments with

565 the SPINE data, segmentation with histogram-based threshold estimation takes ap-
566 proximately 0.035 times real time on a 1 GHz Pentium-III processor with 512 mega-
567 bytes of RAM. This excludes the time taken for computing the KLT-based features,
568 which takes about 0.02 times realtime, but is shared with the recognizer which uses the
569 same features. Segmentation using Gaussian-based threshold detection took about
570 0.025 times realtime in our experiments. It must be noted that these numbers are,
571 however, functions of the width of the averaging window and the length of the segment
572 used for computing histograms.

6. Discussions and conclusions

574 In this paper we have proposed an algorithm for endpointing of speech signals in a
575 continuously recorded signal stream. The segmentation is performed using a combi-
576 nation of classification and clustering techniques by using classifier distributions to
577 project data into a space where clustering techniques can be applied effectively to
578 separate speech and non-speech events. In order to enable effective clustering, the
579 separation between classes is improved by an averaging operation. The performance of
580 the algorithm is shown to be almost comparable to that obtained with manually ob-
581 tained segmentation in moderate and highly noisy speech, as demonstrated by our
582 experiments on the noisy SPINE databases. We note here that a variant of the proposed
583 segmentation algorithm was used by Carnegie Mellon University in both the SPINE1
584 and SPINE2 evaluations, where its overall performance was best amongst all sites that
585 evaluated on a common platform.

586 It must be noted here that the performance obtainable with likelihood-based pro-
587 jections is not completely independent of the match between the classifier distributions
588 and the data. As mentioned earlier, optimal discrimination is only possible in the
589 likelihood space if the distributions used are the true distributions of the classes. As the
590 distributions used for the projections deviate from the true distributions, such guar-
591 antees are no longer valid. In practice, the result of such mismatches is that the modes
592 in the distribution of the likelihood-differences begin to merge, making it increasingly
593 difficult to classify speech frames accurately. Thus it is important, as far as is possible,
594 to attempt to minimize the mismatch between the distributions used for projection and
595 the data. Adapting the distributions to the data may provide some improvement in the
596 performance. However, it must be noted here that even without adaptation, the end-
597 pointer performs extremely well in conditions of small to medium mismatch, such as
598 that between the SPINE2 and SPINE1 data, which differ greatly in the type and level of
599 background noise.

600 The current implementation of the segmenter does not utilize any *a priori* knowledge
601 of the dynamics of the speech signal. Every frame is classified independently of every
602 other frame. We know, for instance, that the performance of a static classifier-based
603 segmenter can be significantly improved by using dynamic statistical models such as
604 HMMs for the classes instead of static models (e.g. Acero *et al.*, 1993). We expect that
605 similar improvements can be achieved in the proposed segmenter as well by including
606 contextual information through a dynamic model, such as an HMM.

607 Rita Singh was sponsored by the Space and Naval Warfare Systems Center, San Diego,
608 under Grant No. N66001-99-1-8905. The content of the information in this publication
609 does not necessarily reflect the position or the policy of the US Government, and no
610 official endorsement should be inferred.

611 References

- 612 Acero, A., Crespo, C., De la Torre, C. & Torrecilla, J. C. (1993). Robust HMM-based endpoint detector.
613 *Proceedings of Eurospeech'93*, pp. 1551–1554.
- 614 Chen, S. & Gopalakrishnan, P. (1998). Speaker, environment and channel change detection and clustering via
615 the Bayesian information criterion. *Proceedings of the Broadcast News Transcription and Understanding*
616 *Workshop*, pp. 127–132.
- 617 Cohen, J. R. (1989). Application of an auditory model to speech recognition. *Journal of the Acoustical Society*
618 *of America* **85**(6), 2623–2629.
- 619 Compennolle, D. V. (1989). Noise adaptation in hidden Markov model speech recognition systems. *Computer*
620 *Speech and Language* **3**(2), 151–168.
- 621 DDVPC (2001). DoD digital voice processing consortium. Available as [http://www.plh.af.mil/ddvpc/](http://www.plh.af.mil/ddvpc/index.html)
622 [index.html](http://www.plh.af.mil/ddvpc/index.html).
- 623 Dempster, A. P., Laird, N. M. & Rubin, D. B. (1977). Maximum likelihood from incomplete data via the EM
624 algorithm (with discussion). *Journal of Royal Statistical Society Series B* **39**, 1–38.
- 625 Doh, S. -J. (2000). *Enhancements to transformation-based speaker adaptation: principal component and inter-*
626 *class maximum likelihood linear regression*. PhD Thesis, Carnegie Mellon University.
- 627 Duda, R. O., Hart, P. E. & Stork, D. G. (2000). *Pattern Classification*, 2nd edition, Wiley, New York.
- 628 Hain, T. & Woodland, P. C. (1998). Segmentation and classification of broadcast news audio. *Proceedings of*
629 *the International Conference on Speech and Language Processing ICSLP98*, pp. 2727–2730.
- 630 Hamada, M., Takizawa, Y. & Norimatsu, T. (1990). A noise-robust speech recognition system. *Proceedings of*
631 *the International Conference on Speech and Language Processing ICSLP90*, pp. 893–896.
- 632 Hirsch, H. G. (1993). Estimation of noise spectrum and its application to SNR estimation and speech
633 enhancement. Tech. Report TR-93-012, International Computer Science Institute, Berkeley, CA.
- 634 Junqua, J.-C., Mak, B. & Reaves, B. (1994). A robust algorithm for word boundary detection in the presence
635 of noise. *IEEE Transactions on Speech and Audio Processing* **2**(3), 406–412.
- 636 Lamel, L., Rabiner, L. R., Rosenberg, A. & Wilpon, J. (1981). An improved endpoint detector for isolated
637 word recognition. *IEEE ASSP Magazine* **29**, 777–785.
- 638 Lasry, M. J. & Stern, R. M. (1984). *A posteriori* estimation of correlated jointly Gaussian mean vectors. *IEEE*
639 *Transactions on Pattern Analysis and Machine Intelligence* **6**, 530–535.
- 640 Leggetter, C. J., & Woodland, P. C. (1994). Speaker adaptation of HMMs using linear regression. Tech.
641 report CUED/F-INFENG/TR. 181, Cambridge University.
- 642 Linguistic Data Consortium (2001). Speech in noisy environments (SPINE) audio corpora. LDC Catalog
643 numbers LDC2001S04, LDC2001S06 and LDC2001S99.
- 644 Rabiner, L. R. & Sambur, M. R. (1975). An algorithm for determining the endpoints of isolated utterances.
645 *Bell Systems & Technical Journal* **54**(2), 297–315.
- 646 Rabiner, M. R. & Juang, B. H. (1993). *Fundamentals of Speech Recognition*. Prentice-Hall Signal Processing
647 Series, Prentice-Hall, Englewood Cliffs, NJ.
- 648 Siegler, M., Jain, U., Raj, B. & Stern, R. M. (1997). Automatic segmentation, classification and clustering of
649 broadcast news audio. *Proceedings of the DARPA ASR Workshop*, pp. 97–99.
- 650 Singh, R., & Raj, B. (2002). Likelihood as a non-linear discriminant projection. Under review.
- 651 Singh, R., Seltzer, M. L., Raj, B., & Stern, R. M. (2001). Speech in noisy environments: robust automatic
652 segmentation, feature extraction, and hypothesis combination. *Proceedings of the IEEE International*
653 *Conference on Acoustics Speech and Signal Processing ICASSP2000*.
- 654 SPINE (2001). Available as <http://eleazar.itd.nrl.navy.mil/spine/spinel/index.html>.
- 655 Viterbi, A. J. (1967). Error bounds for convolutional codes and an asymptotically optimum decoding
656 algorithm. *IEEE Transactions on Information Theory*, 260–269.
- 657
- 658

(Received 2 January 2002 and accepted for publication 12 May 2002)